Published in final edited form as:
Exp Cell Res. 2013 October 15; 319(17): . doi:10.1016/j.yexcr.2013.07.015.

Nrf2 Modulates Contractile and Metabolic Properties of Skeletal Muscle in Streptozotocin-Induced Diabetic Atrophy

Samantha A Whitman[1], **Min Long**[1,2], **Georg Wondrak**[1], **Hongting Zheng**[2,*], and **Donna D. Zhang**[1,*]

[1]Department of Pharmacology and Toxicology, University of Arizona, Tucson, Arizona

[2]Department of Endocrinology, Xinqiao Hospital, Third Military Medical University, Chongqing 400037, PR China

Abstract

The role of Nrf2 in disease prevention and treatment is well documented, however the specific role of Nrf2 in skeletal muscle is not well described. The current study investigated whether Nrf2 plays a protective role in an STZ-induced model of skeletal muscle atrophy.

Modulation of Nrf2 through siRNA resulted in a more robust differentiation of C2C12s, whereas increasing Nrf2 with sulforaphane treatment inhibited differentiation. Diabetic muscle atrophy was not dramatically influenced by Nrf2 genotype, since no differences were observed in total atrophy (all fiber types combined) between WT+STZ and KO+STZ animals. Nrf2-KO animals however, illustrated alterations in muscle size of Fast, Type II myosin expressing fibers. KO+STZ animals show significant alterations in myosin isoform expression in the GAST. Similarly, KO controls mimic both WT+STZ and KO+STZ muscle alterations in mitochondrial subunit expression. PGC-1α, a well-established player in mitochondrial biogenesis and myosin isoform expression, was decreased in KO control, WT+STZ and KO+STZ SOL muscle. Similarly, PGC-1α protein levels are correlated with Nrf2 levels in C2C12s after modulation by Nrf2 siRNA or sulforaphane treatment.

We provide experimental evidence indicating Nrf2 plays a role in myocyte differentiation and governs molecular alterations in contractile and metabolic properties in an STZ-induced model of muscle atrophy.

Keywords

Nrf2; skeletal muscle; atrophy; myosin; metabolism

[*]To whom correspondence should be addressed: dzhang@pharmacy.arizona.edu or htzheng@pharmacy.arizona.edu.
Primary Corresponding Author: Donna Zhang, Ph.D., Pharmacology and Toxicology, College of Pharmacy, University of Arizona, 1703 East Mabel Street, Tucson, AZ 85721, 520-626-9918
Co-Corresponding Author at time of publication: Hongting Zheng, MD, Department of Endocrinology, Xinqiao Hospital, Third Military Medical University, Chongqing 400037, PR China

The authors report no known conflict of interest.

Introduction

Loss of skeletal muscle mass, or atrophy, is a major symptom in a variety of chronic disease states, including denervation, heart failure, cancer and diabetic cachexia. Overall, the contributing players in muscle atrophy control a unique balance between protein synthesis and degradation, namely, hypertrophic pathways involving IGF-1 signaling [1] and proteolytic pathways like the calpain, lysosomal or ubiquitin proteasome (for review, see [2]). Although the precise mechanism of diabetes-induced skeletal muscle atrophy remains unknown, the increased expression of reactive oxygen species (ROS) has been identified as a possible trigger [3].

The transcription factor, Nrf2 (NF-E2-related factor 2) plays a central role in mediating cellular oxidative stress in response to a myriad of stimuli, including environmental toxins, xenobiotics and ROS (for review, see [4]). The Nrf2 pathway is normally kept at low basal levels through interaction with its negative regulator, the ubiquitin substrate adaptor protein, Keap1 (Kelch-like ECH-associated protein 1). Upon stimulation of the pathway through modification of critical cysteine residues on Keap1, Nrf2 is no longer degraded by the 26S proteasome and activates transcription of a barrage of downstream genes. Nrf2 also improves pathological symptoms in conditions like neurodegeneration [5], autoimmune disease [6], diabetes-associated neuropathy [7] and nephropathy [8, 9], as well as contributes to disease prevention.

Most recently, Nrf2 has garnered attention for its potential therapeutic uses in improving kidney function in patients with chronic kidney disease [10], however, the details and safety of the specific drug mechanisms and appropriate patient populations are still being investigated [11]. A multitude of evidence has arisen linking Nrf2 status to the ability to prevent or alleviate diabetic symptoms associated with issues like environmental toxicants (arsenic) [12], cardiovascular dysfunction [13] and insulin action [14, 15]. Yet there remains a gap regarding Nrf2's role in skeletal muscle and its link to pathological muscle wasting or atrophy.

In this study, we investigated how Nrf2 influences myogenic differentiation and utilized a model of STZ-induced diabetic atrophy to determine whether Nrf2 plays a role in protecting skeletal muscle. Our results indicate that Nrf2 activity appears to function in myocyte differentiation. However, Nrf2 genotype alone does not translate into a significant protection from Type-1 diabetic muscle atrophy. What's more, Nrf2 genotype appears to influence other metabolic properties and molecules, particularly in oxidative muscle types such as the Soleus. Specifically, Nrf2 levels are associated with the transcriptional co-activator, PGC-1α, which has been shown to impact muscle fiber-type and mitochondrial biogenesis. Our data support a model where NRF2 is involved in muscle metabolism and alterations in muscle disease and set the foundation for determining Nrf2 pathway linkage to conditions of pathological muscle atrophy.

Materials & Methods

Reagents and Antibodies

Streptozotocin (STZ) was purchased from Sigma (St. Louis, MO). Sulforaphane (D-/L-isomer) was obtained from Santa Cruz Biotechnology, (Santa Cruz, CA). Trizol was purchased from Life technologies (Carlsbad, CA). Blood glucose levels were measured using a Freestyle Lite glucose meter (Abbott Diabetes Care, Inc. Alameda, CA). Urine glucose levels were measured using Diastix (Bayer, Tarrytoen, NY). Serum insulin levels were measured using the Insulin, Mouse ELISA (Mercodia, Winston Salem, NC). Antibodies for Immunoblot and immunofluorescence included: anti-fast skeletal myosin

(clone MY-32, Sigma), anti-dystrophin (Abcam, Cambridge, MA), anti-MyoD or myogenin (BD), anti-total oxphos cocktail (Mitosciences, Eugene, OR), anti-Nrf2, NQO1, Lamin-A and secondary antibodies conjugated to HRP (Santa Cruz Biotechnology). Secondary antibodies conjugated to Alexa Fluor® Dyes for immunofluorescence were purchased from Life Technologies. Antibodies were used at manufacturer instructed dilutions for Immunoblot experiments and diluted to roughly 1μg/mL for immunofluorescence experiments or according to manufacturer's instructions.

Animals

$Nrf2^{+/+}$ (WT) and $Nrf2^{-/-}$ (KO) C57BL/6 mice (described previously [16]) were obtained by breeding homozygous WT or KO mice. All animals received food and water *ad libitum* with the exception of periods required to obtain fasting blood glucose levels. Six-eight week old mice of each genotype were evenly allocated by body weight into two groups (N=4-6/group). Animals in each group received either sodium citrate (Control) or STZ (50 mg/kg, pH 4.5, dissolved in sodium citrate) through intraperitoneal (i.p.) injection for 5 consecutive days. Two weeks following STZ injection, both urine and fasting glucose levels (FGL, four hour fast) were measured. Mice with a FGL and urine glucose level above 250 mg/dL and 500 mg/dL, respectively were considered diabetic and used for this study. Diabetic mice were euthanized for final data analysis four-weeks after establishment of diabetes. The University of Arizona Institutional Animal Care and Use Committee approved all animal work and protocols.

Cell Culture and Treatments

Mouse derived myoblasts, C2C12 cells were obtained from the ATCC and maintained in growth media (GM, DMEM + 10% Fetal Bovine Serum) at low passage numbers (<25) under 65% confluence. For differentiation studies, C2C12s were grown to >90% confluence and media was changed to differentiation media (DM, DMEM + 2% horse serum). C2C12s were treated with compounds to induce Nrf2 activation (sulforaphane (SF) (2 μM) for 4 hours before cell harvest and analysis. Nrf2 siRNA was obtained from Qiagen and transfected following manufacturer instructions using the HiPerfect kit (Qiagen). Cells were harvested in SDS sample buffer (62.5 mM Tris, pH 6.8, 5% wt/vol SDS, 10% vol/vol glycerol, 5% vol/vol 2-mercaptoethanol, and 0.02% wt/vol bromphenol blue) for protein analysis.

Tissue and Sample Preparation

At the time of euthanasia and tissue harvest, skeletal muscles (gastrocnemius (GAST) orsoleus (SOL)) from each animal were isolated from the right hind limb and placed in Optimum Cutting Temperature (OCT medium) (Tissue-Tek) for histological analysis. GAST and SOL muscles from the left hind limb were ground to a homogenous powder over liquid N_2. Portions of the powdered samples were set aside for either RNA analysis (~15 μg) or were solubilized for protein expression analysis in Urea sample buffer (8M Urea, 2M Thiourea, 3% SDS, 75mM DTT, 0.05M Tris-HCl, 0.03% bromophenol blue, 50% glycerol with Leupeptin, E-64, and PMSF inhibitors). Protein lysates were cleared from debris and stored at -80°C for analysis.

Analysis of Tissue Oxidative Stress

Skeletal muscle samples were analyzed in an indirect assessment of oxidative stress using the Thiobarbituric Acid Reactive Substances (TBARS) assay kit from Cayman Chemical. Powdered tissue sample of the GAST was solubilized in RIPA buffer (50 mM Tris-HCl, pH 7.6, containing 150 mM sodium chloride, 1% NP-40, 0.5% sodium deoxycholate, and 0.1% SDS) with protease inhibitors. The assay was then carried out according to manufacturer

instructions and analyzed by reading absorbance at 540 nm. Standards provided in the kit were used to generate a standard curve and unknown values of MDA expression were extrapolated from the standard values. Data is represented as concentration of MDA (in μM) per dry weight of total GAST tissue (in mg).

RNA Expression Analysis

Briefly, RNA isolation and gene expression analysis was conducted according to the MIQE guidelines [17]. Total RNA were isolated from GAST and SOL tissues using Trizol. RNA quality was assessed on a Nanodrop (Wilmington, DE) where the 260/280 ratio was obtained. Samples with a ratio of 1.7-2.1 were processed for downstream gene analysis. Approximately 500ng total RNA from each sample was reverse transcribed using M-MLV (Promega, Madison, WI), oligoDT, random primers and dNTPs from Roche (Indianapolis, IN) (see online materials Table S1). cDNA was diluted ~1:20 in nuclease free water to be used for qPCR. For most targets, gene expression levels were analyzed using SYBR green chemistry (KAPA Biosciences), except for the myosin heavy chain genes and β-actin. Due to similarities in myosins, for additional specificity, we utilized TaqMan chemistry with primers and probes designed in Roche's Universal Probe Library Design Center. All experiments were conducted on a LightCycler 480 (Roche). Relative gene expression was calculated using the $2^{-\Delta\Delta CT}$ method [18]. For all housekeeping and target genes assessed, standard curves were evaluated on 10-fold serial dilutions of control skeletal muscle cDNA to determine reaction efficiency. Where efficiencies differed >5%, efficiencies could be accounted for in the LightCycler 480 software during analysis of relative gene expression. A complete list of target genes and primers is provided in the online materials (Table S2). Specificity of primer pairs were evaluated by in-run Melt curve analysis and the use of both genomic DNA and water template control samples. Only primers that did not amplify more than one product (by Melt curve) or any product in the genomic and water controls were used for final experiments.

Immunofluorescence

Skeletal muscle mounted in OCT was sectioned (5 μm) on a cryostat microtome in cross. Muscle sections were fixed in 100% ice-cold MeOH and incubated with primary antibodies diluted in 5%BSA/0.05% Tween-20/PBS at room temperature (RT) for ~4 hours. Samples were washed extensively at RT in PBS + 0.2% Tween-20 then incubated with appropriate secondary antibodies for 1 hour at RT, washed extensively, rinsed in ddH_2O and mounted using Gelvatol. Sections were probed with single or a dual detection using anti-myosin and anti-dystrophin to determine fiber type and cross-sectional area of the same cross-section. Species-specific secondary antibodies directly conjugated with Alexa Fluor® 488 or 594 were used to detect primary antibodies (~1 μg/mL).

Muscle Cross-sectional Area

Images were taken from immunofluorescence experiments co-detecting dystrophin and fast skeletal myosin on a Zeiss Observer.Z1 using a Zeiss FLUAR 10×/0.5NA air objective and Slidebook 5.0 software. Serial images were taken of each muscle sample (GAST or SOL) to ensure the entire cross section was represented for each animal. Images were analyzed in a pipeline created in CellProfiler [19], which is provided in the supplemental materials (Fig. S1).

Myosin Heavy Chain Isoform Expression, Electrophoresis and Immunoblots

Protein lysates were subjected to SDS-PAGE using 8% acrylamide (acrylamide:bisacrylamide ratio: 37.5:1) gels with a 4% acrylamide stack, and were run for 24 hours at 4°C at a constant 275 V. Gels were stained with a standard coomassie protocol.

MyHC isoform was determined by its migratory pattern (see Wada et al. [20]). Gels were scanned to a digital copy and NIH Image J software was used to analyze relative MyHC isoform content by densitometry.

For other protein expression analysis, lysates were subjected to SDS-PAGE using gels ranging from 7.5 – 12% to reach appropriate resolution for the desired molecular weight. Gels were transferred to nitrocellulose membranes and subjected to immunoblot analysis. Blots were blocked in 5% milk in PBS, contacted with primary antibodies at manufacturer instructed dilutions, washed in PBS+ 0.1% Tween-20, contacted with appropriate anti-rabbit, -mouse or –goat secondary antibodies conjugated to HRP (Santa Cruz), washed and signals were detected using SuperSignal West Dura or Femto Chemiluminescent Substrate (Thermo Scientific). Molecular weights of target proteins were determined by their relative migration to the PageRuler™ prestained protein ladder (Fermentas).

Statistical Analyses

Results are expressed as mean ± SD. Statistical tests were performed using StatPlus software. Unpaired Student's *t* tests were used to compare the means of two groups. One-way ANOVA was applied to compare the means of three or more groups using Tukey-Kremer post-hoc analysis to determine which group exhibited differences. $P < 0.05$ was considered to be significant. For qPCR experiments, results are expressed as relative gene expression compared to a housekeeping gene (ODC or β–actin). Relative expression less than 0.5-fold or greater than 2-fold (1 cycle difference) is considered noteworthy and potentially biologically relevant.

Results

Modulation of Nrf2 influences myotube differentiation

To first interrogate how Nrf2 might influence skeletal muscle, Nrf2 activity and levels were manipulated. To activate Nrf2, C2C12 myocytes were treated with sulforaphane (SF), an isothiocyanate, which releases the basal Nrf2 inhibition by Keap1. On the other hand, to inactivate Nrf2, its levels were decreased by treatment with an Nrf2 siRNA. Treated C2C12s were taken through a standard differentiation procedure by switching from growth media ((GM) used to maintain myoblasts) to differentiation media ((DM) used to induce myotube formation) over a 48h time period. Notably, in Fig. 1A, treating C2C12s with Nrf2 siRNA to reduce Nrf2 levels resulted in increased expression of the myogenic transcription factors MyoD and Myogenin, as well as Myosin Heavy Chain (MyHC). In Fig. 1A and 1B, the Western blot for Nqo1 (a downstream Nrf2 target gene) is provided to help demonstrate the effectiveness of the Nrf2 siRNA, furthermore, densitometry graphs for Nrf2 protein levels have been provided in Fig. 1C. As expected, increasing Nrf2 levels by SF treatment of C2C12s prior to differentiation yielded opposing results to that of treatment by Nrf2 siRNA. Activation of the Nrf2 pathway with SF appeared to inhibit or delay myotube differentiation (Fig. 1B) as noted by a decrease in MyoD, Myogenin and Myosin expression. Together, these data indicate that alteration of Nrf2 levels through either SF activation or siRNA dramatically impacts the progression of myotube differentiation in C2C12 cells.

Nrf2 influences slow muscle fiber pathways

To expand on the C2C12 studies and Nrf2s ability to modulate myocyte differentiation, we sought to investigate how Nrf2 levels affect a muscle atrophy model of Type I diabetes using STZ injection. Fig. 2 shows that Nrf2 WT+STZ and KO+STZ animals did acquire diabetes, as expected, and showed equivalent increases in their fasting blood glucose (Fig. 2A), reduction of serum insulin levels (Fig. 2B) and body weight loss over the 6-week study period (Fig. 2C). To address the reduction in basal serum insulin levels of Nrf2 KO mice,

these mice are known to be more susceptible to damage of the pancreatic islets and a 45% reduction in serum insulin levels in naive Nrf2 KO mice has been described previously by Dr. Klaassen's group [21].

Subsequent analysis of the STZ animal models were conducted on gastrocnemius (GAST) and soleus (SOL) muscles, which represent two muscle types that are different in their metabolic and contractile properties, (i.e., “fast/glycolytic” and “slow/oxidative,” respectively). To further characterize this animal model, mRNA levels of Nrf2 and its key downstream target genes were examined in GAST and SOL muscles from each experimental animal group. First, analysis of *Nrf2* revealed no alteration in its mRNA levels in WT animals with STZ-induced diabetes (Fig. 2D) when compared to WT alone. Analysis of Nrf2 mRNA shows the KO animals are in fact null for *Nrf2* message. Compared to WT control animals, the common downstream target gene, *Nqo1*, is elevated only in the SOL of WT+STZ animals but is markedly down regulated in KO control and KO+STZ animals (Fig. 2E), whereas other Nrf2 downstream genes, *Gclm* and *Hmox1* (HO-1) are unaltered regardless of Nrf2 genotype or treatment (Fig. 2F and 2G). These data suggest that there is minimal oxidative stress occurring in muscles undergoing diabetic atrophy as a result of STZ treatment, with the exception of elevated *Nqo1* in the SOL of WT+STZ animals.

To interrogate more specifically the oxidative stress levels in the muscle, GAST samples underwent analysis by TBARS assay. Formation of highly reactive and unstable lipid hydroperoxides and decomposition derived from polyunsaturated fatty acids lead to malondialdehyde (MDA) accumulation, which is measured in the TBARS assay. Results indicate a mild increase in oxidative stress in the WT+STZ group (non-significant compared to WT control) and significant increases in the KO animals, regardless if STZ treatment (Fig. 2H). These data indicate, that the skeletal muscle is experiencing oxidative stress, despite the minimal rise in Nrf2 downstream genes observed by qPCR.

Diabetic muscle atrophy is not dramatically affected by Nrf2 status

To assess whether the observed loss of body weight in WT+STZ and KO+STZ animal groups was attributable to muscle atrophy, cross-sectional area (CSA) of the GAST and SOL were assessed. Fig. 3A provides representative images of frozen GAST in cross-section, stained with an anti-dystrophin antibody to mark the outer membrane of the myofibers. Both Nrf2 WT+STZ and KO+STZ animals exhibited a significant decrease in CSA of the GAST (Fig. 3B). Though the KO+STZ animals trended to be smaller that the WT+STZ, this trend was not statistically significant. The reduction in muscle size was also reflected in total GAST dry weight (Fig. 3C), where interestingly, the KO control animals trended toward a reduced muscle mass when compared with WT controls that was not reflected in the CSA data. Total SOL CSA (all fiber types combined) was significantly reduced in WT+STZ and KO+STZ groups (Fig. 3D), with a trend towards a smaller total CSA in KO control animals that did not reach significance. As an extension of the CSA data, mRNA levels of players involved in atrophy, including muscle E3-ligases, Murf1 (*Trim63*) and Atrogin-1 (*Fbx32*), or the calcinuerin pathway were analyzed. *Trim63* was elevated in both GAST and SOL of WT+STZ and KO+STZ animals (Fig. 3E). However, *Fbx32* showed elevation in only the GAST of WT+STZ animals, but increased in both the GAST and SOL of KO+STZ mice (Fig. 3F). No alterations of calcinuerin A (*Pppc3a*) were observed (Fig. 3G). Of note, muscle transcription factors myogenin and MyoD were up regulated in both WT+STZ and KO+STZ animals (Fig. 3H), however, only MyoD was up in the KO control muscle, supporting some of the findings in vitro that low levels of Nrf2 equate to increases in myogenic transcription factors. Taken together, these data suggest that Nrf2 genotype does not have a dramatic impact on total muscle loss due to diabetes, but appears to have more minor effects on expression of E3-ligases in certain (particularly slow,

oxidative) muscles, as well as some influence on major myogenic transcription factors (MyoD).

Myosin Heavy Chain (MyHC) Isoform Expression in muscle is altered by Nrf2 genotype

Given the findings of differential gene expression between the GAST and SOL muscle, (*Nqo1* and *Fbx32*), we investigated further metabolic and contractile property differences with these muscle types by analyzing myosin heavy chain (MyHC) subtypes. MyHC isotype expression is also subject to alterations based on disease state and activity levels [22, 23]. Similar to the total CSA analysis in Fig. 3, frozen sections from SOL were also co-stained with an anti-fast myosin antibody (clone MY-32) to demarcate fiber type differences between MyHC type I, or "slow" and MyHC Type II, or "fast" (Fig. 4A and Supplemental Fig. S2). Both WT+STZ and KO+STZ groups showed significant reduction in fiber CSA regardless of muscle fiber type or myosin expression (Fig. 4B). However, the KO control animals displayed a significantly smaller CSA in their "fast," Type II myosin expressing fibers when compared to WT control, which could account for the trend in the total muscle CSA.

Fig. 5A shows representative images taken from lanes of a low percentage SDS gel to determine MyHC distribution in muscles from our animals. The resulting data show that diabetes caused a shift in MyHC type in the GAST from MyHC IIa to MyHC IIb/x only in KO+STZ animals ($P < 0.05$), whereas the WT+STZ group actually trended (though non-significant) toward a shift in the opposite direction (Fig. 5B). Interestingly, Nrf2 genotype did not influence overall MyHC expression patterns in the SOL. However, all animals treated with STZ (both WT and KO) showed a marked shift in MyHC expression from the faster, type IIa isoform towards a slower type I (Fig. 5C). These data are supported by qPCR analysis of the different MyHC genes, *Mhy1, 2*, and *7* corresponding to MyHC IIx, IIa, and I, respectively (data not shown).

Given the alterations in MHC distribution in the SOL of STZ treated animals and the unique alterations to MHC isoform expression in the GAST of the KO+STZ animals, we briefly interrogated mitochondrial subunit expression as an indication of corresponding metabolic alterations. Interestingly, as Table 1 illustrates, changes were observed in the relative distribution of mitochondrial subunits as reflected by representative protein levels via Western Blot (OxPhos antibody cocktail, Mitosciences). Specifically, the KO control animals exhibit changes to their mitochondrial subunit expression that mimic those of both WT+STZ and KO+STZ animals. Additionally, certain changes observed for the SOL, such as increases in the ATP producing Complex V, are in contrast to variations in the GAST where a decrease in Complex V was seen. Also, KO+STZ mice frequently illustrate more severe alterations than the WT+STZ animal group, particularly for changes observed in the GAST. Overall, the data suggest that diabetes and Nrf2 KO mice change levels of Complex V by increases in the SOL and decreases in the GAST. What's more, Complex I, which is known for its contributions to reactive oxygen species, are altered only in the KO control and KO+STZ animals. In summary, Nrf2 genotype appears to alter not only MyHC expression and fiber type profiles, but also inherent metabolic properties as represented by mitochondrial subunit expression in KO control mice and mice with type I diabetes.

PGC-1α expression is affected by Nrf2 status

The transcriptional co-regulator, peroxisome proliferator-activated receptor gamma coactivator 1alpha, (PGC-1α) is central to influencing muscle metabolism, myosin isoform and mitochondrial biogenesis. We investigated the potential of PGC-1α involvement in the alterations to Nrf2 WT and KO muscles in these studies. Analysis of mRNA expression of PGC-1α (*Ppargc1a*) was markedly decreased in the SOL muscle in KO control animals as

well as both WT+STZ and KO+STZ groups (Fig. 6A). Expanding on this observation, the influence of Nrf2 status on PGC-1α protein levels was further interrogated in C2C12s treated with either Nrf2 siRNA or the activating compound, SF. Fig. 6B illustrates that, similar to the findings in the Nrf2 KO SOL, when Nrf2 levels are reduced by siRNA, so are PGC-1α protein levels. Conversely, activation of Nrf2 with SF in C2C12s shows a corresponding increase in PGC-1α protein levels (Fig. 6C). In summary, these data reveal that the KO control (STZ untreated) animals mimic both WT and KO diabetes groups by displaying a notable reduction of PGC-1α transcript in their SOL muscle, which suggests inherent genotype differences in muscle metabolism even without diabetes. Additionally, Nrf2 levels appear to influence PGC-1α protein levels in a positive correlation in C2C12 cells.

Discussion

The therapeutic benefits of Nrf2 activation as well as the requirements of Nrf2 in disease prevention have been well documented in several disease states. To date, the specific role of Nrf2 in protection from skeletal muscle atrophy has not been investigated. In the present study, we hypothesized that the anti-oxidant regulator, Nrf2, would have a role in protection against muscle atrophy in a model of STZ-induced diabetes. Surprisingly, Nrf2 genotype did not dramatically influence total skeletal muscle atrophy as measured by cross-sectional area. However, subtler genotype alterations were found when investigating molecular and metabolic alterations of STZ-induced skeletal muscle atrophy. Specifically, Nrf2 KO mice showed trends toward lower muscle weights, displayed significant atrophy of Fast muscle fibers in the SOL, displayed alterations in MyHC isotype and mitochondrial subunit expression and a reduction in PGC-1α. In addition, modulation of Nrf2 in a myocyte culture model illustrates that Nrf2 status is tightly linked to the timing of myogenic differentiation.

Although Nrf2 KO mice did not suffer significantly worse muscle atrophy (when assessing total CSA, regardless of muscle fiber type) associated with STZ-induced diabetes, our results show an interesting requirement of Nrf2 in the fine-tuning of metabolic and contractile property shifts seen with STZ-induced diabetes. Specifically, Nrf2 KO mice displayed unique alterations to mitochondrial subunit expression, muscle size and MyHC content specifically of fast, Type II muscles, such as the GAST. These results are somewhat surprising, given the inherent metabolic properties of these muscle types, relying primarily on glycolysis and not oxidative phosphorylation. Although indirect measurements of oxidative stress were assessed in the GAST (TBARS), these data show a blunted response in the WT+STZ animals. It is possible this is a result of the Nrf2 pathway scavenging ROS and conferring protection, as indicated by the up regulation of *Nqo1* mRNA in the WT+STZ group only. Direct measurements of ROS activity in each muscle type (GAST vs. SOL) would be beneficial in understanding the potential role of ROS feedback to the Nrf2 pathway, and how this may signal alterations in muscle metabolism.

Interestingly, ROS is a required second messenger for myocyte differentiation [24], but the role of ROS in pathological muscle conditions remains controversial, with many reports suggesting high levels of ROS contribute to muscle pathology rather than regeneration (for review, see [25]). Our data suggest that modulation of Nrf2 as early as in myoblasts can dramatically alter the differentiation program. One possibility is that increasing Nrf2 (and thus scavenging ROS prior to differentiation cues), inhibits or delays differentiation. An observation of our current data is that Nrf2 protein levels appear to decrease in differentiated C2C12s when compared to undifferentiated cells maintained in growth media. It is possible that undifferentiated myoblasts maintain higher levels of Nrf2 for tighter regulation of ROS signaling for differentiation. Future studies could explore this phenomenon further in the context of Nrf2's role in muscle repair in adult/differentiated muscle versus a satellite cell

population of reserve/undifferentiated myocytes. Of note, the ability to scavenge ROS and handle oxidative stress is dramatically reduced in the muscles of Nrf2 KO animals. What's more, alterations in mitochondrial subunits were notable in that they demonstrated the strongest Nrf2 genotype differences amongst all of the molecular profiles that were investigated in this study. More work should be done to expand on the potential functional changes that these molecular mitochondrial profiles might induce. Specifically, linking subunit expression levels to enzymatic activity, ROS production and overall metabolic changes to substrate utilization of the muscle would be valuable data. In addition, more work needs to be conducted to investigate the intimate timing of Nrf2 activation and how this may affect different muscle pathologies, such as disuse atrophy versus diabetic or cancer cachexia.

Another important pathway triggered by ROS is that leading to the up regulation of PGC-1α. The PGC-1α transcriptional coactivator is a major regulator of energy metabolism [26] that controls many aspects of oxidative metabolism, including mitochondrial adaptations, glucose transport, oxidative phosphorylation and myosin isoform expression. PGC-1α is selectively expressed in slow-twitch fibers in skeletal muscle and ectopic expression of the PGC-1α gene in either a cell or an animal has been shown to promote fast to slow fiber-type switch [27]. Interestingly, our data support Nrf2 being upstream of PGC-1α expression, although other myogenic factors, such as MEF-2, are currently documented in the literature as being prime regulators of PGC-1α in muscle [28]. Regarding the similarities in PGC-1α levels between STZ treated groups and Nrf2 KO control animals, it is reported that Nrf2 levels are down regulated in cardiac muscle in diabetes [29]. Though our studies do not have this direct evidence, there is precedence that diabetes can reduce Nrf2 in striated muscle tissues, which could account for the similarities between the KO control and STZ animals. Also, our data appear to differ with data reported in the literature [27], as the SOL muscle in our STZ-induced diabetes muscle transitions from MyHC II to MyHC I and displays reduced, rather than increased PGC-1α levels. One possibility could be the use of STZ to induce diabetes. Previous work has demonstrated a potential influence of STZ on muscle atrophy that is independent of other genetic models accounting for diabetic atrophy effects [30]. Our observations of fiber type shifting being antagonistic to PGC-1α levels could be attributed to alterations brought on by STZ, however, more extensive work in several genetic or diet induced models of diabetes would need to be conducted.

Collectively, our findings support the first model where Nrf2 is involved in “fine-tuning” the skeletal muscle response to STZ-induced muscle atrophy. Though Nrf2 genotype was not dramatically involved in gross morphology changes, (i.e., it was unable to illustrate protection from total muscle atrophy), Nrf2 appears to be required for preventing detrimental shifts in MHC isoform and metabolic alterations that might contribute to disease pathology. This study lays important groundwork to further investigate the role of Nrf2 in molecular alterations to critical muscle contractile and metabolic properties that may be applied in therapeutic intervention for diseases involving disuse or cachexia based muscle atrophy.

Supplementary Material

Refer to Web version on PubMed Central for supplementary material.

Acknowledgments

This study was supported by R01ES015010 and R01CA154377 (National Institutes of Health) to D.D.Z. and 81228023 (National Natural Science Foundation of China) to D.D. Z. and H.Z. Dr. Donna D Zhang is the guarantor of this work and, as such, had full access to all the data in the study and takes responsibility for the integrity of the

data and the accuracy of the data analysis. The Authors would like to thank Wang Tian, Huihui Wang and Hui Li (all affiliated with University of Arizona, Dept. of Pharmacology & Toxicology) for assistance with pilot studies. S.W., Y.Z. and H.Z. researched data. G.W and H.Z contributed to discussion, and provided critical reagents. S.W. and D.Z. wrote manuscript.

References

1. Sacheck JM, Ohtsuka A, McLary SC, Goldberg AL. IGF-I stimulates muscle growth by suppressing protein breakdown and expression of atrophy-related ubiquitin ligases, atrogin-1 and MuRF1. American journal of physiology Endocrinology and metabolism. 2004; 287:E591–601. [PubMed: 15100091]
2. Jackman RW, Kandarian SC. The molecular basis of skeletal muscle atrophy. American Journal of Physiology - Cell Physiology. 2004; 287:C834–C843. [PubMed: 15355854]
3. Aragno M, Mastrocola R, Catalano MG, Brignardello E, Danni O, Boccuzzi G. Oxidative Stress Impairs Skeletal Muscle Repair in Diabetic Rats. Diabetes. 2004; 53:1082–1088. [PubMed: 15047625]
4. Ma Q. Role of nrf2 in oxidative stress and toxicity. Annual review of pharmacology and toxicology. 2013; 53:401–426.
5. Burton NC, Kensler TW, Guilarte TR. In vivo modulation of the Parkinsonian phenotype by Nrf2. Neurotoxicology. 2006; 27:1094–1100. [PubMed: 16959318]
6. Ma Q, Battelli L, Hubbs AF. Multiorgan autoimmune inflammation, enhanced lymphoproliferation, and impaired homeostasis of reactive oxygen species in mice lacking the antioxidant-activated transcription factor Nrf2. The American journal of pathology. 2006; 168:1960–1974. [PubMed: 16723711]
7. Negi G, Kumar A, Sharma SS. Melatonin modulates neuroinflammation and oxidative stress in experimental diabetic neuropathy: effects on NF-kappaB and Nrf2 cascades. Journal of pineal research. 2011; 50:124–131. [PubMed: 21062351]
8. Zheng H, Whitman SA, Wu W, Wondrak GT, Wong PK, Fang D, Zhang DD. Therapeutic potential of Nrf2 activators in streptozotocin-induced diabetic nephropathy. Diabetes. 2011; 60:3055–3066. [PubMed: 22025779]
9. Cui W, Bai Y, Miao X, Luo P, Chen Q, Tan Y, Rane MJ, Miao L, Cai L. Prevention of diabetic nephropathy by sulforaphane: possible role of Nrf2 upregulation and activation. Oxidative medicine and cellular longevity. 2012; 2012:821936. [PubMed: 23050040]
10. Pergola PE, Raskin P, Toto RD, Meyer CJ, Huff JW, Grossman EB, Krauth M, Ruiz S, Audhya P, Christ-Schmidt H, Wittes J, Warnock DG. Bardoxolone methyl and kidney function in CKD with type 2 diabetes. The New England journal of medicine. 2011; 365:327–336. [PubMed: 21699484]
11. Zoja C, Corna D, Nava V, Locatelli M, Abbate M, Gaspari F, Carrara F, Sangalli F, Remuzzi G, Benigni A. Analogues of Bardoxolone Methyl Worsen Diabetic Nephropathy in Rats with Additional Adverse Effects. American journal of physiology Renal physiology. 2012
12. Yang B, Fu J, Zheng H, Xue P, Yarborough K, Woods CG, Hou Y, Zhang Q, Andersen ME, Pi J. Deficiency in the nuclear factor E2-related factor 2 renders pancreatic beta-cells vulnerable to arsenic-induced cell damage. Toxicology and applied pharmacology. 2012; 264:315–323. [PubMed: 23000044]
13. Li B, Liu S, Miao L, Cai L. Prevention of diabetic complications by activation of Nrf2: diabetic cardiomyopathy and nephropathy. Experimental diabetes research. 2012; 2012:216512. [PubMed: 22645602]
14. Wang X, Wu H, Chen H, Liu R, Liu J, Zhang T, Yu W, Hai C. Does insulin bolster antioxidant defenses via the extracellular signal-regulated kinases-protein kinase Bnuclear factor erythroid 2 p45-related factor 2 pathway? Antioxidants & redox signaling. 2012; 16:1061–1070. [PubMed: 22149292]
15. Yu ZW, Li D, Ling WH, Jin TR. Role of nuclear factor (erythroid-derived 2)-like 2 in metabolic homeostasis and insulin action: A novel opportunity for diabetes treatment? World journal of diabetes. 2012; 3:19–28. [PubMed: 22253942]
16. Moi P, Chan K, Asunis I, Cao A, Kan YW. Isolation of NF-E2-related factor 2 (Nrf2), a NF-E2-like basic leucine zipper transcriptional activator that binds to the tandem NF-E2/AP1 repeat of the

beta-globin locus control region. Proceedings of the National Academy of Sciences of the United States of America. 1994; 91:9926–9930. [PubMed: 7937919]

17. Bustin SA, Benes V, Garson JA, Hellemans J, Huggett J, Kubista M, Mueller R, Nolan T, Pfaffl MW, Shipley GL, Vandesompele J, Wittwer CT. The MIQE guidelines: minimum information for publication of quantitative real-time PCR experiments. Clinical chemistry. 2009; 55:611–622. [PubMed: 19246619]
18. Pfaffl MW. A new mathematical model for relative quantification in real-time RT-PCR. Nucleic acids research. 2001; 29:e45. [PubMed: 11328886]
19. Lamprecht MR, Sabatini DM, Carpenter AE. CellProfiler: free, versatile software for automated biological image analysis. BioTechniques. 2007; 42:71–75. [PubMed: 17269487]
20. Wada M, Hamalainen N, Pette D. Isomyosin patterns of single type IIB, IID and IIA fibres from rabbit skeletal muscle. Journal of muscle research and cell motility. 1995; 16:237–242. [PubMed: 7559996]
21. Aleksunes LM, Reisman SA, Yeager RL, Goedken MJ, Klaassen CD. Nuclear factor erythroid 2-related factor 2 deletion impairs glucose tolerance and exacerbates hyperglycemia in type 1 diabetic mice. The Journal of pharmacology and experimental therapeutics. 2010; 333:140–151. [PubMed: 20086057]
22. Diffee GM, Kalfas K, Al-Majid S, McCarthy DO. Altered expression of skeletal muscle myosin isoforms in cancer cachexia. American Journal of Physiology - Cell Physiology. 2002; 283:C1376–C1382. [PubMed: 12372798]
23. Gosker HR, van Mameren H, van Dijk PJ, Engelen MP, van der Vusse GJ, Wouters EF, Schols AM. Skeletal muscle fibre-type shifting and metabolic profile in patients with chronic obstructive pulmonary disease. The European respiratory journal: official journal of the European Society for Clinical Respiratory Physiology. 2002; 19:617–625.
24. Piao YJ, Seo YH, Hong F, Kim JH, Kim YJ, Kang MH, Kim BS, Jo SA, Jo I, Jue DM, Kang I, Ha J, Kim SS. Nox 2 stimulates muscle differentiation via NF-kappaB/iNOS pathway. Free radical biology & medicine. 2005; 38:989–1001. [PubMed: 15780757]
25. Barbieri E, Sestili P. Reactive oxygen species in skeletal muscle signaling. J Signal Transduct. 2012; 2012:982794. [PubMed: 22175016]
26. Choi CS, Befroy DE, Codella R, Kim S, Reznick RM, Hwang YJ, Liu ZX, Lee HY, Distefano A, Samuel VT, Zhang D, Cline GW, Handschin C, Lin J, Petersen KF, Spiegelman BM, Shulman GI. Paradoxical effects of increased expression of PGC-1alpha on muscle mitochondrial function and insulin-stimulated muscle glucose metabolism. Proceedings of the National Academy of Sciences of the United States of America. 2008; 105:19926–19931. [PubMed: 19066218]
27. Lin J, Wu H, Tarr PT, Zhang CY, Wu Z, Boss O, Michael LF, Puigserver P, Isotani E, Olson EN, Lowell BB, Bassel-Duby R, Spiegelman BM. Transcriptional co-activator PGC-1 alpha drives the formation of slow-twitch muscle fibres. Nature. 2002; 418:797–801. [PubMed: 12181572]
28. Chang JH, Lin KH, Shih CH, Chang YJ, Chi HC, Chen SL. Myogenic Basic Helix-Loop-Helix Proteins Regulate the Expression of Peroxisomal Proliferator Activated Receptor-γ Coactivator-1α. Endocrinology. 2006; 147:3093–3106. [PubMed: 16527841]
29. Tan Y, Ichikawa T, Li J, Si Q, Yang H, Chen X, Goldblatt CS, Meyer CJ, Li X, Cai L, Cui T. Diabetic downregulation of Nrf2 activity via ERK contributes to oxidative stress-induced insulin resistance in cardiac cells in vitro and in vivo. Diabetes. 2011; 60:625–633. [PubMed: 21270272]
30. Krause MP, Riddell MC, Gordon CS, Imam SA, Cafarelli E, Hawke TJ. Diabetic myopathy differs between Ins2Akita+/, àí and streptozotocin-induced Type 1 diabetic models. Journal of Applied Physiology. 2009; 106:1650–1659. [PubMed: 19246652]

Highlights

- Loss of the transcription factor Nrf2 causes molecular alterations in muscle.
- Nrf2 knockout mice show disruptions in mitochondrial subunit expression.
- A diabetic model of muscle atrophy illustrates Nrf2 loss alters myosin expression.
- Nrf2 may influence PGC-1α expression, affecting muscle metabolism and regulation.

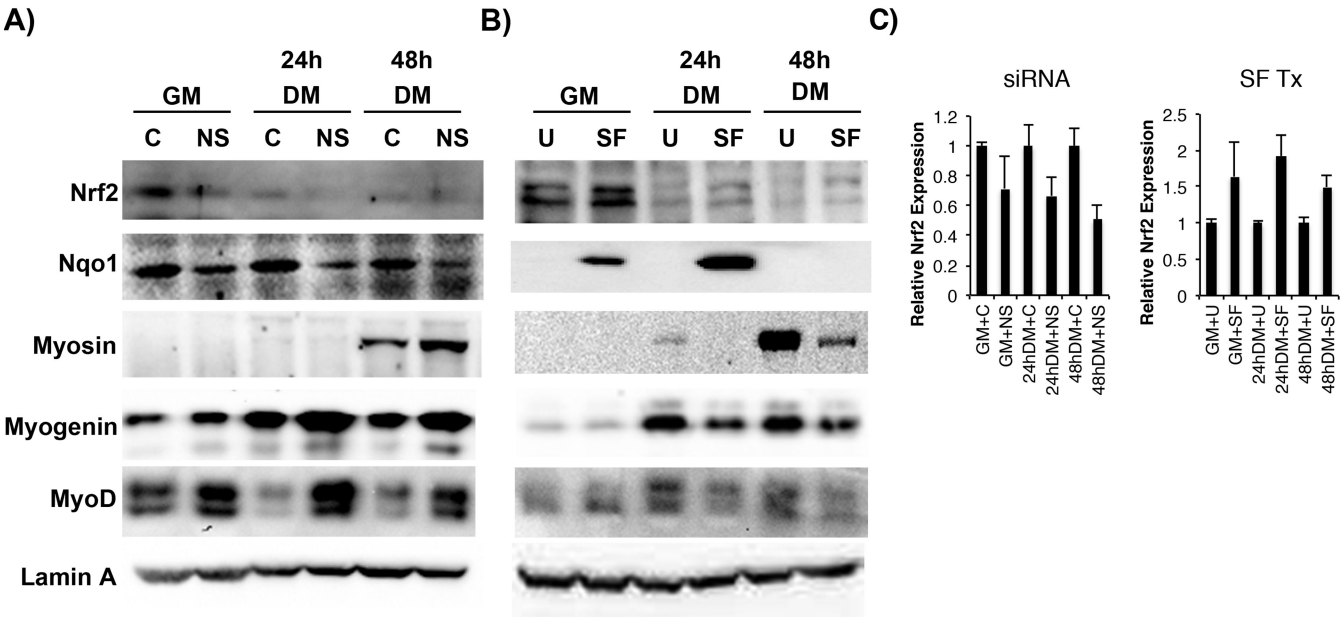

Figure 1. Modulation of Nrf2 influences myotube differentiation

Mouse myoblast C2C12 cells were treated with Nrf2 siRNA and analyzed by 10% SDS-PAGE (A). Myoblasts were cultured in growth media (GM) or differentiation media (DM) at 24 and 48h after treatment with scrambled control siRNA (C) or Nrf2 specific siRNA (NS). In (B) C2C12 cells were untreated (U) or treated with 2μM Sulforaphane (SF) every 24h and samples analyzed by 7.5% SDS-PAGE. Western Blot analysis of Nrf2 and downstream target, Nqo1 illustrate effects of siRNA or SF treatment. Markers of myogenic differentiation include transcription factors MyoD and Myogenin and the contractile protein, Myosin. Densitometry analysis of Nrf2 Westerns (C) help to illustrate protein level changes wit siRNA or SF treatment. Data indicate a negative correlation between Nrf2 level and degree of myocyte differentiation.

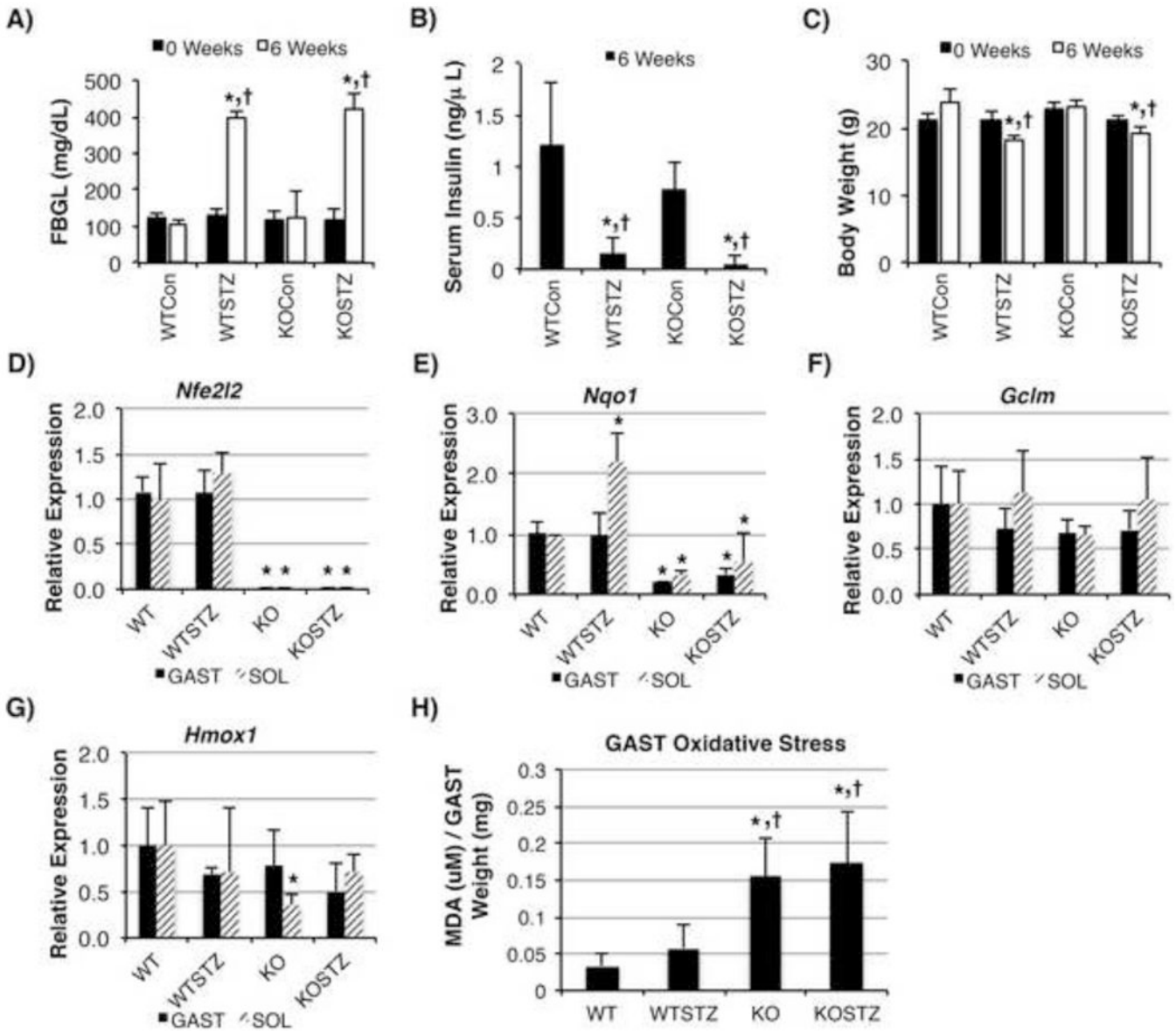

Figure 2. Establishment of STZ-induced Diabetes in Nrf2 mouse model; Nrf2 influences slow muscle fiber pathways

Nrf2 WT or KO mice were given STZ to induce diabetes. Fasting blood glucose levels (FBGL) (A)), serum insulin levels (B) and total body weight (C) illustrate both WT and KO mice establish diabetes. Relative mRNA expression levels (setting WT control to 1) are displayed for *Nfe2l2* (Nrf2) (D)), *Nqo1* (E), *Gclm* (F) and *Hmox-1* (HO-1) (G)). Oxidative stress (H) was analyzed by TBARS assay. For A-C, * = $p < 0.05$ compared to WT control, † = $p < 0.05$ compared to KO control; N=4-6 animals/group. For D-G, * = denotes fold change greater than 2-fold compared to WT control; N=3-6 animals/group. For H, * = $p < 0.05$ compared to WT control, † = $p < 0.05$ compared to WT+STZ; N=4 animal/group.

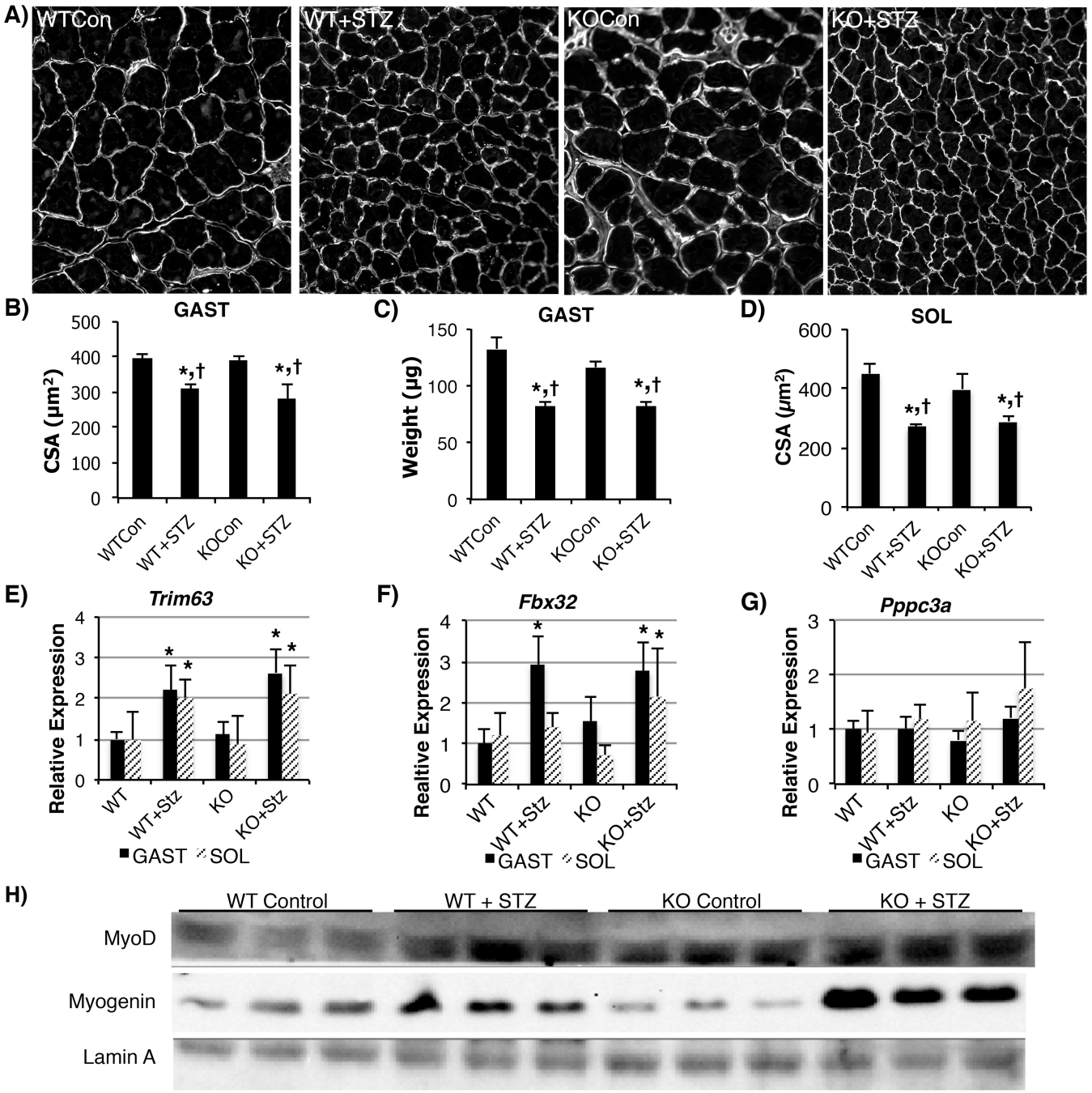

Figure 3. Diabetic muscle atrophy is not dramatically affected by Nrf2 status

Representative images (A) of Gastrocnemius muscle (GAST) stained with dystrophin to mark the membranes, which were used to determine muscle cross sectional area (CSA). Average GAST CSA for each animal group (B) (Average ~2,500 fibers/animal). Dry GAST muscle weight (C) shows trend toward reduction in KO control and significant reduction in WT+STZ and KO+STZ. Total CSA from Soleus (SOL) (D) show similar decrease in muscle size to GAST. Relative mRNA expression of proteolytic genes *Trim63* (Murf1) (E), *Fbx32* (Atrogin-1) (F) and *Ppp3ca* (Calcineurin-A) from GAST and SOL muscles. Representative Western blots (H) for MyoD and Myogenin from animal SOL samples illustrate an increase in MyoD expression in WT+STZ, KO control and KO+STZ. Lamin A was used as a loading

control. For B-D, * = $p < 0.05$ compared to WT control, † = $p < 0.05$ compared to KO control; N=4-6 animals/group. For E-G, * = denotes fold change greater than 2-fold compared to WT control; N=3-6 animals/group.

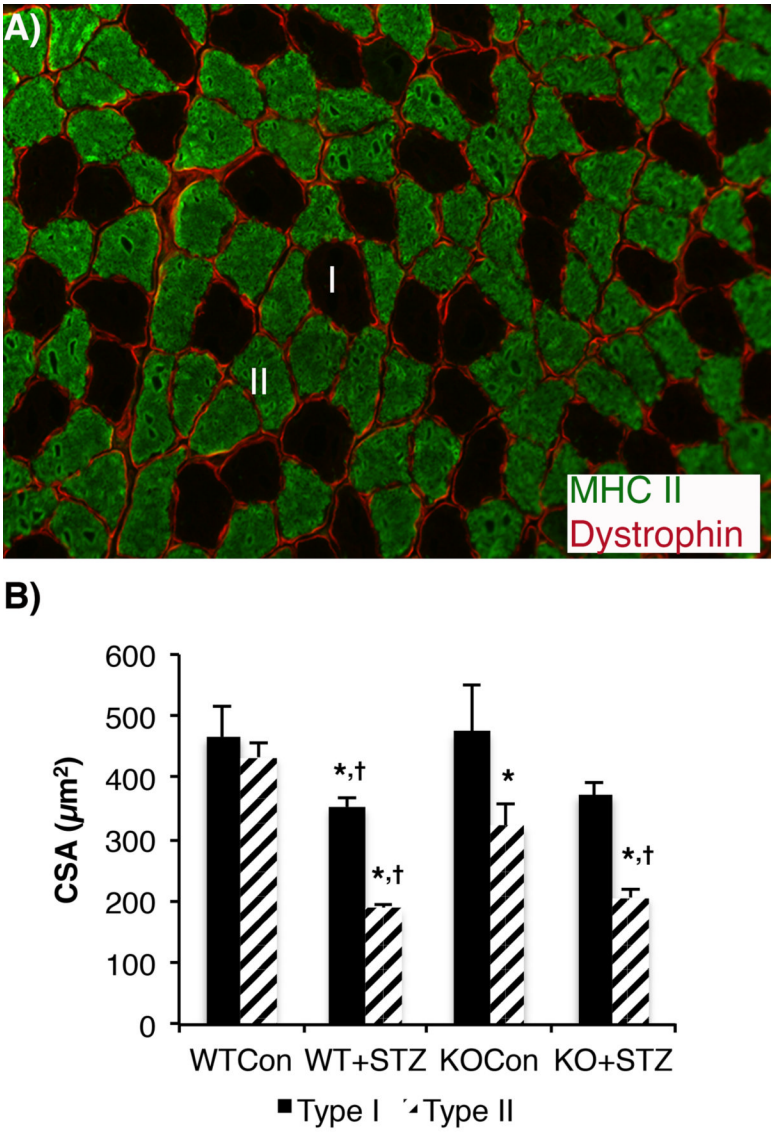

Figure 4. Fast muscle fiber size of the Soleus is influenced by Nrf2 genotype

Frozen SOL muscle was doubled labeled with dystrophin (red) to mark membranes and myosin heavy chain (MHC) II (green) for fast, glycolytic fibers (representative image A). Average CSA by SOL fiber type is displayed in (B). WT+STZ and KO+STZ have significant reduction in area of both fiber types whereas KO control animals show significant reduction in Type II fibers. * = $p < 0.05$ compared to WT control, † = $p < 0.05$ compared to KO control; N=4-6 animals/group.

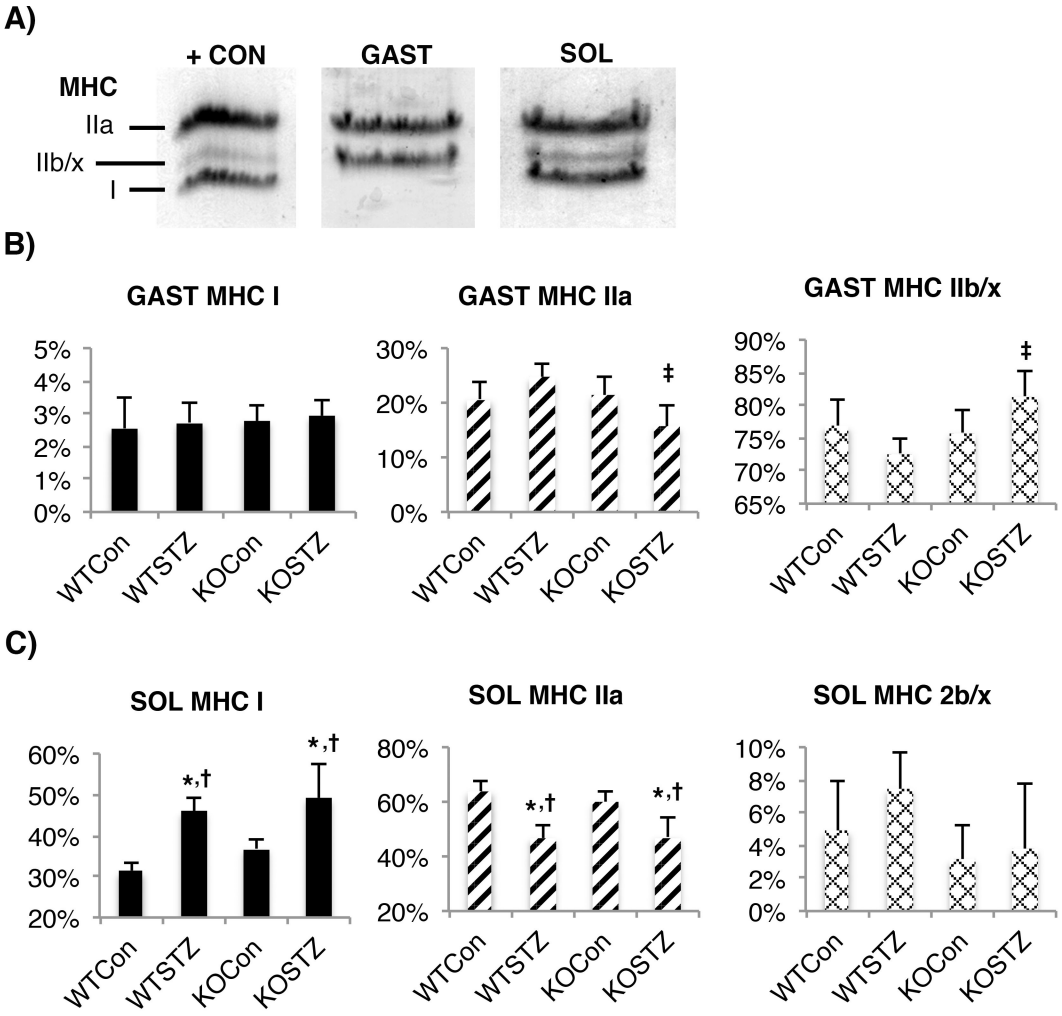

Figure 5. Myosin Heavy Chain (MyHC) Isoform Expression in muscle is altered by Nrf2 genotype

Representative lanes from 8% SDS gels used to separate myosin (MHC) isoforms I (slow), IIa (intermediate-fast) and IIb/x (fast) (A). Relative densitometry of each myosin isoform from the GAST (B) and the SOL (C) show alterations between animal groups. Only KO +STZ animals show a significant shift from myosin type IIa towards IIb/x in the GAST when compared to WT+STZ animals. Both WT+STZ and KO+STZ have significant shifts in fiber types of the SOL from IIa towards I. * = $p < 0.05$ compared to WT control, † = $p < 0.05$ compared to KO control, ‡ = $p > 0.05$ compared to WT+STZ; N=4-6 animals/group.

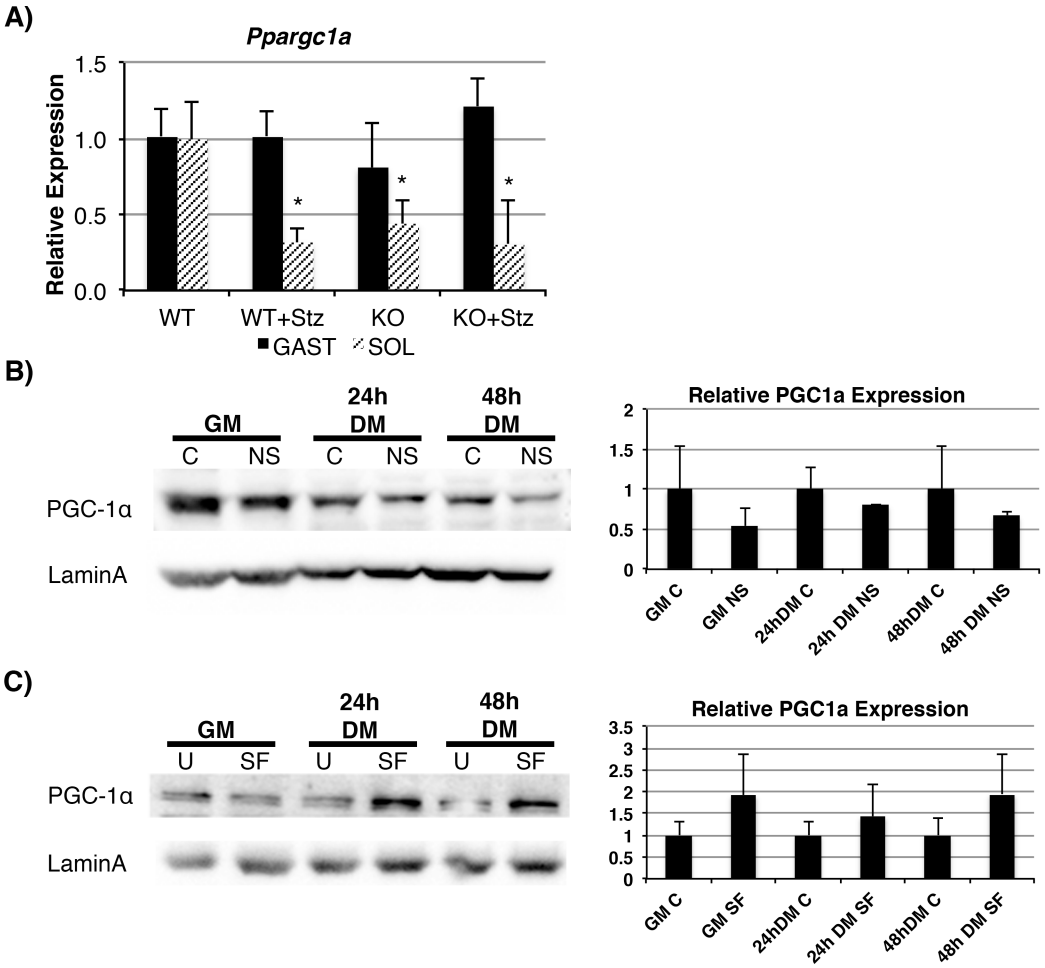

Figure 6. PGC-1α expression is affected by Nrf2 status

Relative mRNA expression of *Ppargc1a* (PGC-1α) is significantly reduced in the SOL of KO control, WT+STZ and KO+STZ animals (A). In (B) PGC-1α protein levels correspond to Nrf2 levels, when Nrf2 is reduced by siRNA ("NS"), compared to scramble control siRNA ("C"). Conversely, increasing Nrf2 levels through treatment with Sulforaphane (SF) in (C) increases PGC-1α levels above cells that are untreated (U). Myoblasts were cultured in growth media (GM) or differentiation media (DM) at 24 and 48h. Densitometry analysis of (B) and (C) provide relative expression of PGC-1α levels across treatment and time.

Table 1

Expression of Mitochondrial subunits in Soleus is altered in Nrf2-/- mice. Whole muscle lysates were separated by SDS-PAGE, transferred to nitrocellulose and reacted with the OxPhos monoclonal antibody cocktail (Mitosciences) to investigate the relative expression of mitochondrial subunits in both Soleus and Gastrocnemius muscles.

SOLEUS	WT Con	WT+STZ	KO Con	KO+STZ
Complex V (ATP5A)	0.12 ± 0.02	0.19 ± 0.04 *	0.24 ± 0.01 *	0.23 ± 0.02 *
Complex IV (MTCO1)	0.50 ± 0.03	0.37 ± 0.07 *	0.35 ± 0.06 *	0.35 ± 0.01 *
Complex III (UQCRC2)	0.18 ± 0.02	0.25 ± 0.06 *	0.25 ± 0.01	0.26 ± 0.01 *
Complex II (SDHB)	0.08 ± 0.03	0.09 ± 0.01	0.10 ± 0.04	0.09 ± 0.01
Complex I (NDUFB8)	0.12 ± 0.01	0.11 ± 0.01	0.07 ± 0.01 *†	0.07 ± 0.01 *†
GASTROC				
Complex V (ATP5A)	0.35 ± 0.33	0.35 ± 0.03	0.26 ± 0.03	0.24 ± 0.08 *†
Complex IV (MTCO1)	0.34 ± 0.05	0.33 ± 0.02	0.30 ± 0.02	0.26 ± 0.04 *
Complex III (UQCRC2)	0.17 ± 0.01	0.15 ± 0.02	0.17 ± 0.01	0.21 ± 0.02 †
Complex II (SDHB)	0.08 ± 0.01	0.09 ± 0.01	0.11 ± 0.02 *	0.16 ± 0.02 *†$
Complex I (NDUFB8)	0.07 ± 0.04	0.09 ± 0.01	0.16 ± 0.03 *†	0.14 ± 0.01 *†

* = $p < 0.05$ compared to WT Con,

† = $p < 0.05$ compared to WT+STZ.